H_K = height of fluidization reactor, m
Δp = pressure drop, Pa
T = absolute temperature, °K
U_f = superficial fluid velocity, m · s^{-1}

Greek Letters

ϵ = bed voidage
ϵ_p = bed voidage obtained by pouring particles
ψ = particle sphericity
μ = viscosity, Pa · s
ν = kinematic viscosity, m^2 · s^{-1}
ρ = density, kg · m^{-3}

Dimensionless Groups

Re_{mf} = $U_{mf}\, d_p/\nu_g$ particle Reynolds number at minimum fluidization velocity
Ga = $\bar{d}_p^3\, \rho_g\, \rho_s\, g/\mu_g^2$ Galilei number

Subscripts

calc = value computed from theoretical equation
exp = value determined experimentally
g = gas property
mb = property at minimum bubbling point of a gas
mf = property at minimum fluidization point
s = property of solid particle

LITERATURE CITED

Broadhurst, T. E., and H. A. Becker, "Onset of Fluidization and Slugging in Beds of Uniform Particles," *AIChE J.*, **21**, 238 (1975).

Desai, A., H. Kikukawa, and A. H. Pulsifer, "The Effect of Temperature Upon Minimum Fluidization Velocity," *Powder Technol.*, **16**, 143 (1977).

Doheim, M. A., and C. N. Collinge, "Effect of Temperature on Incipient Fluidization and Study of Bed Expansion," *Powder Technol.*, **21**, 289 (1978).

Ergun, S., "Fluid Flow Through Packed Column," *Chem. Eng. Prog.*, **48**, 89 (1952).

Saxena, S. C., and G. J. Vogel, "The Measurement of Incipient Fluidization Velocities in a Bed of Coarse Dolomite at Temperature and Pressure," *Trans.*, Instn. Chem. Engr., **55**, 184 (1977).

Sosna, M. C., and N. B. Kondukov, "Criteria and Correlation for Computation of Minimum Fluidization Velocity of Polydispersion Particle Beds," in Russian, *Inzh. Fiz. Zhurnal*, **15**, 73 (1968).

Syromjatnikov, N. I., and V. F. Volkov, "Fluidized Bed," in Russian, Metallurgizdat, Sverdlovsk (1959).

Manuscript received June 9, 1980; revision received October 9, and accepted October 21, 1980.

A Technique for Computer Simulation of Time Varying Slag Flow in a Coal Gasification Reactor

S. R. GOLDMAN

Jaycor, Del Mar, CA 92014

Slag is produced in a slagging coal gasification reactor when devolatilized coal particles burn and leave a residue of molten ash. The ash particles can impinge on the reactor wall and form a film of slag flowing down along the sides of the reactor (Hoy et al., 1965). The flow poses a limit on proper operation in that it can be so great as to plug the tap hole at the bottom of the reactor (Figures 1 and 2).

Although various special cases can be used to estimate the thickness of the slag layer (Bird et al., 1960), computer simulation suggests itself as a means for removing the uncertainty in the estimates as well as for such purposes as determining the heat transport through the slag at all wall locations and the treatment of time varying behavior.

The basic equations determining slag flow are:

$$\frac{\partial \vec{v}}{\partial t} + \vec{v} \cdot \nabla \vec{v} = -\nabla p/\rho + \nabla \cdot (\nu \nabla \vec{v}) + \vec{g} \tag{1}$$

$$\nabla \cdot \vec{v} = 0 \tag{2}$$

$$\frac{\partial y_b}{\partial t} + u_b \frac{\partial y_b}{\partial x} = v_b + S_a \tag{3}$$

$$\frac{\partial T}{\partial t} + \vec{v} \cdot \nabla T = \frac{1}{\rho C_v} \nabla \cdot (k \nabla T). \tag{4}$$

The unknowns are $\vec{v}$, T, p and y_b. For azimuthally symmetric flow, the independent spatial coordinates for the boundary layer are x and y. As one moves along the wall, the x and y axes rotate.

We use the boundary layer approximation (Landau and Lifshitz, 1959):

$$\delta y/\delta x < 1. \tag{5}$$

We note $\rho_1 = Re\ \delta y/\delta x$, whereas $\rho_2 = Re\ Pr\ \delta y/\delta x$.

As an illustration, we consider a reactor with a slag flow rate of 0.1 kg/s, an effective radius at the tap hole of 7.5×10^{-2} m, and ash with characteristics: $k = 1.5$ J/(m · s · °K), $\rho = 2.5 \times 10^3$ kg/m^3, $C_v = 1.8 \times 10^3$ J/kg · °K, $\mu = 1.90 \times 10^8 \exp(-1.07 \times 10^{-2}\, T)$ kg/m · s for $I > I_f$(=1583°K). At T = 1922°K

$$\rho_1 = 0.97\ \delta y/\delta x \tag{6}$$

and

$$\rho_2 = 2.5 \times 10^2\ \delta y/\delta x. \tag{7}$$

From Eqs. 5 and 6, $\rho_1 < 1$; yet simultaneously from Eq. 7, unless $\delta y/\delta x \lesssim 4 \times 10^{-3}$, $\rho_2 > 1$. Hence we set the left hand side of Eq. 1 equal to zero, but we retain the left hand side of Eq. 4. Essentially we are recognizing the condition: $Pr > 1$.

To lowest order in y making use of Eq. 5, we have $h_1 = 1$, $h_2 = 1$, and $h_3 = r - y \cos\theta$. The form for h_3 allows consistently for finite y/r.

For simulational convenience we use variables x', y', and t' so that:

$$\frac{\partial}{\partial t} = \frac{\partial}{\partial t'} - \frac{y'}{y_b} \frac{\partial y_b}{\partial t'} \frac{\partial}{\partial y'} \tag{8}$$

$$\frac{\partial}{\partial x} = \frac{\partial}{\partial x'} - \frac{y'}{y_b} \frac{\partial y_b}{\partial x'} \frac{\partial}{\partial y'} \tag{9}$$

$$\frac{\partial}{\partial y} = \frac{1}{y_b} \frac{\partial}{\partial y'}. \tag{10}$$

On using Eqs. 5 and 8-10, Eqs. 1-4 can be rewritten in conservative form:

$$0 = -\frac{1}{\rho} \frac{\partial p}{\partial x'} + \frac{1}{h_3 y_b^2} \frac{\partial}{\partial y'} \left(\nu h_3 \frac{\partial u}{\partial y'} \right) + g \cos\theta \tag{11}$$

S. R. Goldman is presently with Los Alamos National Laboratory, Los Alamos, NM 87545.

0001-1541-81-4818-0869-$2.00

©The American Institute of Chemical Engineers, 1981.

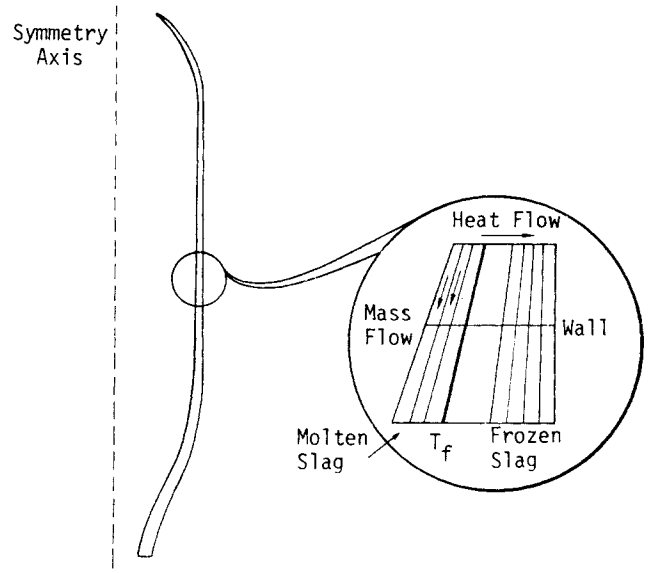

Figure 1. Schematic simulation geometry. Each slag zone (roughly 10 cm high × 0.1 cm thick) has its own temperature, viscosity and flow velocity.

$$\frac{\partial}{\partial y'}(h_3 v) = -\frac{\partial}{\partial x'}(y_b h_3 u) + \frac{\partial}{\partial y'}\left(y' h_3 u \frac{\partial y_b}{\partial x'}\right) \tag{12}$$

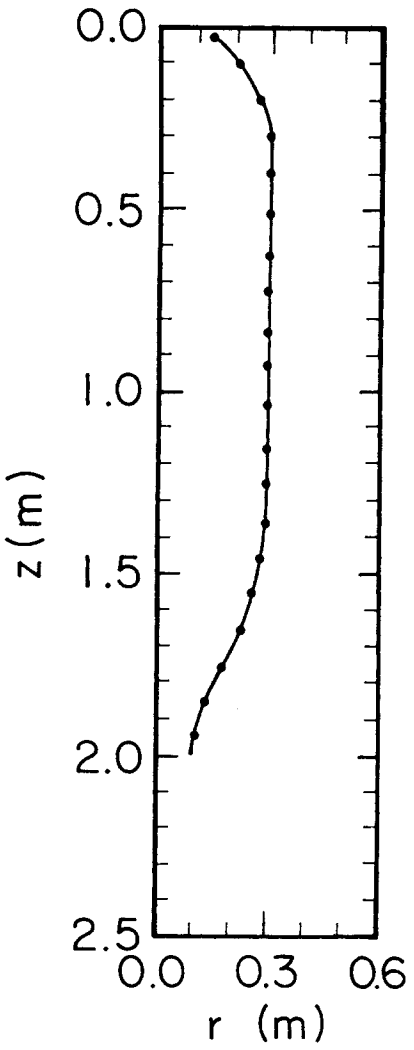

Figure 2. Specific reactor geometry. Tick marks denote centers of cell locations in x.

$$\frac{\partial}{\partial t'}\left[\left(r - \frac{y_b}{2}\cos\theta\right)y_b\right] + \frac{\partial}{\partial x'}\int_0^1 dy'\, y_b h_3 u = -\alpha_a v_a (r - y_b \cos\theta) \tag{13}$$

$$\frac{\partial}{\partial t'}(h_3 y_b T) + \frac{\partial}{\partial x'}(h_3 u y_b T) + \frac{\partial}{\partial y'}\left(h_3 v T - \frac{\partial y_b}{\partial t'} h_3 y' T - u \frac{\partial y_b}{\partial x'} h_3 y' T\right) = \frac{1}{\rho C_v}\frac{\partial}{\partial y'}\left(\frac{k}{y_b} h_3 \frac{\partial T}{\partial y'}\right). \tag{14}$$

[In Eqs. 11-14 an azimuthal swirl velocity (which could be accounted for in parallel to u) has been systematically neglected. In the boundary layer approximation $\partial p/\partial y' < \partial p/\partial x'$ so that $\partial p/\partial x = \partial p/\partial x'$.]

From Eq. 13 it is clear that the mass flux due to ash particles is $-\alpha_a v_a$. This assumes that the ash particles are in the molten state and that they stick to the slag layer surface. The heat flux to the slag film has the form:

$$\sigma\epsilon(T_a^4 - T_{sb}^4) - \rho c_v T_a \alpha_a v_a + h_{gs}(T_a - T_{sb}). \tag{15}$$

The term in $\sigma\epsilon$ is due to radiation transport. The term in T_a is due to ash particles impinging on the slag. The term in h_{gs} is due to heat conduction through the boundary layer *between* the gas proper and the slag.

One can solve for the equations numerically in the following manner:

1. The physical region of slag is divided into a grid of dimension NX by NY. The cells are uniformly spaced in x' and y'. Boundary conditions at the minimum and maximum values of x' are accounted for by two extra layers of cells at fixed x' and $0 \leq y' \leq 1$. Hence the dimension of the computational mesh is $(NX + 2)$ by NY.

2. Values for $T(I,J)$ and $y_b(I)$ are specified at $t' = 0$ (or the beginning of a time step).

3. Finite difference equations for Eqs. 11-14 are obtained by integrating over the cell centered around (I,J). First, Eq. 11 is solved for u. (In the boundary layer approximation $\partial p/\partial x'$ is determined solely from the gas flow field.) Then, Eq. 12 is solved for v. Then the Courant condition time step for the entire mesh is found by taking the minimum Courant time step over all locations for Eqs. 13 and 14, with boundary layer conduction and radiation transport terms at $y' = 1$ treated implicitly in Eq. 14. (In particular, for radiation transport, the term in $T_a^4 - T_{sb}^4$ is factored into linear and cubic terms with the value of T_{sb} in the linear term treated implicitly.) Then, Eq. 13 is stepped forward in time for $(r - y_b \cos\theta/2)y_b$ and hence for $y_b(I)$. Then, Eq. 14 is stepped forward in time for $h_3 y_b T$ and hence for $T(I,J)$. The time step is then complete and Eq. 11 can be solved again.

4. Eqs. 13 and 14 are differences by the second upwind method (Roache, 1976).

5. Although there is no temporal variation in Eq. 12 the differencing in the three terms there should be the same as the differencing for the corresponding three terms in Eq. 14. Hence the terms in Eq. 12 are also treated by upwind differencing. Physically this is necessary to ensure that a completely isothermal problem remains isothermal. Numerically, it was found that if the differencing was not the same for the two equations, temperature inhomogeneities were driven numerically. These then coupled with the strong dependence of viscosity on temperature to produce breakdowns in the solution procedure. No such behavior was observed once the differencings in Eqs. 12 and 14 were made identical.

Numerical results for $NX = 20$ and $NY = 10$ were obtained for the unit of Figure 2 with slag from Rosebud No. 7 coal with a slag flow rate/diameter of 0.66 kg/s · m. The reactor gas was taken to

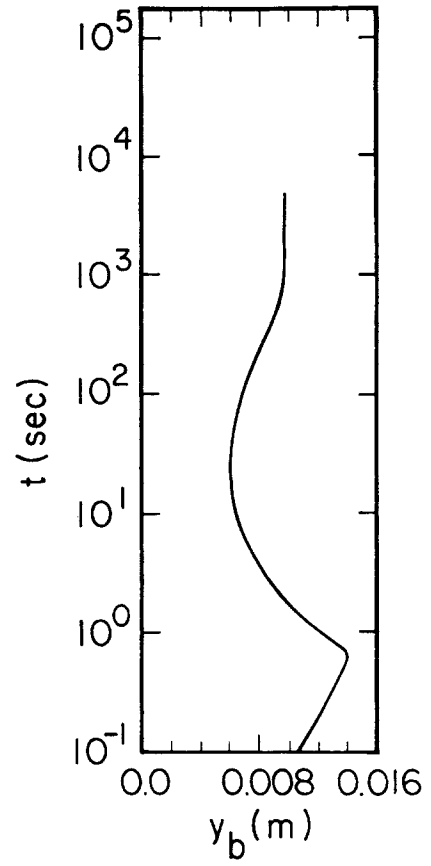

Figure 3. Slag layer thickness at the tap hole as a function of time.

be at 1922°K. A uniform conductance was taken between the slag surface at the vessel wall and cooling tubes containing water at 500°K. The behavior for cells within the reactor was virtually independent of boundary conditions specified by the imaginary row of cells at $I = 1$ (the top of the reactor). The combination of upwind differencing and the downward slag flow ensured that the values for y_b and T at $I = NX + 2$ (the imaginary row of cells at the bottom of the reactor) did not affect values for $I \leq NX + 1$.

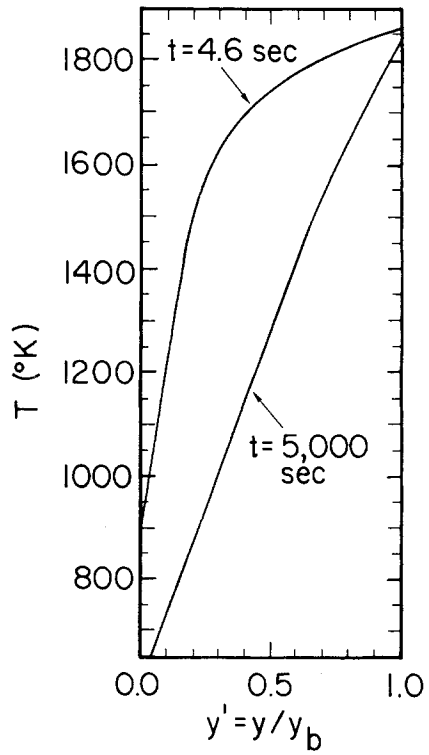

Figure 4. Temperature profiles within the boundary layer at the tap hole.

The initial slag layer was taken to be 10^{-2} m thick and at a uniform temperature of 1800°K. The slag layer thickness at the top hole as a function of time is shown in Figure 3. The rapid behavior at times of order 1 s is a function of the initial conditions. It is interesting to note that although the criterion $\rho_1 < 1$ was violated at times less than 1 second the algorithm was unaffected in terms of convergence. The slag transient behavior over the entire time interval of calculation is plausible. A substantial amount of the slag present initially runs out of the reactor before cooling, first raising the thickness of the layer at the tap hole above the steady state value and then lowering it. As the stationary temperature gradient develops the mean viscosity of the layer increases and the thickness (with a constant ash source) increases.

The temperature profiles for the boundary layer at the tap hole at 4.6 s and 5000 s are shown in Figure 4. The results at 4.6 seconds indicate control of the temperature field by convection and initial conditions in the time varying temperature Eq. 4. The shallowness of the temperature gradient in y' for $0.5 \leq y' \leq 1.0$ is a reflection of this. The results at 5000 s are explained for the most part by a linear temperature gradient derived from steady state considerations taking into account that the ratio of the liquid slag thermal conductivity (above 1583°K) to the frozen slag thermal conductivity (below 1583°K) was assumed to be 1.44. The lower temperatures at this time compared to the earlier time are due to the choice of $T = 1800$°K for all locations at $t = 0$ and the relatively slow, yet ultimately dominant, effect of thermal diffusion. However, the transient variations could be significant for realistic reactor performance.

In typical cases the results for y_b at the slag tap hole did not vary by more than 10% between runs with $NX = 6$, $NY = 6$ and runs with $NX = 20$, $NY = 10$. For $NX = 20$, $NY = 10$ after 5000 seconds in real time the fractional error in mass conservation was 5.2×10^{-10} and the fractional error in energy conservation was 1.6×10^{-3}; the corresponding running time on a CDC 7600 with a nonoptimized program was 78.5 seconds.

This technique offers a physically fundamental, easily applicable, means for determining in detail time varying slag flow and the associated thermal transport for coal gasification reactors. As such it is directly useful for design calculations (which are vitally concerned with free flow through the tap hole) and as a component within more complex reactor models. It provides self-consistent laminar models which could furnish background conditions for yet more detailed fluid dynamic analyses of slag flow-field stability.

ACKNOWLEDGMENT

It is a pleasure to thank my colleagues at JAYCOR for numerous helpful questions, comments and suggestions. Essential slag parameters and a steady state analysis were first shown to the author by Dr. J. A. Stirling of Phillips Petroleum Co. This work was supported by subcontract from Phillips Petroleum Co. under U.S. Dept. of Energy Contract No. EF77-C-01-1207 to Bituminous Coal Research Inc. The work will be incorporated in a reactor model now being developed for Stearns-Roger Inc.

NOTATION

C_r = temperature-dependent slag specific heat
$\vec{g}$ = gravitational acceleration
h_1, h_2, h_3 = scale factors for x, y and ϕ, respectively
h_{gs} = heat conductance for the boundary layer between gas proper and slag
I = integer denoting discretized cell location in x' ($1 \leq I \leq NX + 2$ including boundary location at $I = 1$ and $I = NX + 2$)
J = integer denoting discretized cell location in y' ($1 \leq J$

$\leq NY$)

k = temperature dependent slag thermal conductivity
NX = number of physical cells in x'
NY = number of physical cells in y'
p = slag pressure
Pr = slag Prandtl number
$r(x')$ = distance of vessel wall from symmetry axis
Re = $\rho u\ \delta y/\mu$ = Reynolds number for the flow layer
S_a = $-\alpha_a(x)\ v_a(x)$ = source term from slag impinging on the boundary layer
t = time
t' = t
$T(x,y,t)$ = slag temperature
T_a = temperature of ash impinging on slag
T_f = slag freezing temperature below which there is no flow
T_g = reactor gas temperature
T_{sb} = $T[x,y_b(x,t),t]$
u = component of $\vec{v}(x,y,t)$ in the x-direction
$u_b(x)$ = velocity of the boundary in the x-direction
v = component of $\vec{v}(x,y,t)$ the the y-direction
$\vec{v}(x,y,t)$ = slag velocity
$v_a(x)$ = ash velocity normal to the slag layer
$v_b(x)$ = velocity of the boundary in the y-direction
x = coordinate denoting arc length along the wall in a vertical plane passing through the combustion chamber axis of symmetry
x' = x
y = coordinate normal to the wall in a vertical plane through the combustion chamber symmetry axis
$y_b(x,t)$ = boundary layer thickness
y' = $y/y_b(x,t)$

Greek Letters

α_a = ash volume fraction in gas adjacent to slag
δx = scale length for variation in x
δy = scale length for variation in y
ϵ = slag emissivity, ($\epsilon \simeq 0.5$)
$\theta(x)$ = angle between the local direction of the x-axis and the vertical
μ = temperature dependent dynamic viscosity
ν = temperature dependent slag kinematic viscosity
ρ = slag density
ρ_1 = ratio of convective to viscous terms in Eq. 1
ρ_2 = ratio of thermal convective to thermal diffusive terms in Eq. (4)
σ = Stefan-Boltzmann constant
ϕ = azimuthal reactor angle
∇ = the nabla or del operator (Bird et al., 1960)

LITERATURE CITED

Bird, R. B., W. E. Stewart, and E. N. Lightfoot, *Transport Phenomena*, John Wiley and Sons, Inc., New York (1960).

Hoy, H. R., A. G. Roberts, and D. M. Wilkens, "Behavior of Mineral Matter in Slagging Gasification Processes," *J. of Institution of Gas Engineers*, **5**, 444 (1965).

Landau, L. D., and E. M. Lifshitz, *Fluid Mechanics*, p. 145, Addison-Wesley Publishing Co., Inc., Reading, MA (1959).

Roache, P. J., *Computational Fluid Dynamics*, p. 73, Hermosa Publishers, Albuquerque, NM (1976).

Manuscript received July 10, 1980; revision received October 20, and accepted October 24, 1980.

Heat Transfer to Laminar In-Tube Flow of Pseudoplastic Fluids

S. D. JOSHI

and

A. E. BERGLES

Department of Mechanical Engineering and Engineering Research Institute
Iowa State University
Ames, IA

This note considers the problem of heat transfer to laminar flow of pseudoplastic fluids in circular tubes with constant heat flux. The constitutive relation for pseudoplastic fluids is $\tau = K(\partial u/\partial y)^n$, with $n \leq 1.0$. Analytical solutions are available for constant property, fully developed flow, e.g., Grigull (1956). Numerical solutions have been presented for developing flow for selected values of n, e.g., McKillop (1964). In both regions, pseudoplastic fluids have higher heat transfer coefficients than Newtonian fluids. Mizushina et al. (1967), Cochrane (1969), and Mahalingam et al. (1975) report analyses which indicate that the temperature dependence of K further increases heat transfer coefficients for heating; however, their predictions are not sufficient for a general correlation.

Results of an efficient explicit numerical solution are presented here. A correlation of these results includes non-Newtonian and temperature-dependent K effects for entrance and fully developed regions.

S. D. Joshi is presently with Phillips Petroleum Co., Bartlesville, OK.

0001-1541-81-4814-0872-$2.00.

©The American Institute of Chemical Engineers, 1981.

PROBLEM FORMULATION AND SOLUTION

In formulating the equations, the following assumptions were made:

1. The flow is steady and axisymmetric.
2. Axial conduction is negligible.
3. Free convection effects are negligible.
4. The usual boundary layer approximations are valid since pseudoplastic fluids exhibit flat velocity and temperature profiles near the tube centerline and sharp profile gradients near the wall.
5. K is temperature-dependent according to the constitutive equation of most industrial fluids:

$$K = a \exp[-bt] \tag{1}$$

With these assumptions, the general governing equations in cylindrical coordinates (Figure 1) reduce to
Momentum (x-direction):

$$\rho u \frac{\partial u}{\partial x} + \rho v \frac{\partial u}{\partial y} = -\frac{dp}{dx} + \frac{1}{r}\frac{\partial}{\partial y}(r\tau) \tag{2}$$